

Charged Higgs contribution to rare top-quark decay $t \rightarrow b\bar{b}bW^+$

S. Slabospitskii^a

^a*NRC “Kurchatov Institute” - IHEP, Protvino, Moscow Region, Russia*

Abstract

The calculation of the rare t -quark decay $t \rightarrow b\bar{b}bW^+$ within the Standard Model as well as the charged Higgs contribution to this decay is presented. The role of possible background processes is discussed. It is shown that this decay provides an additional possibility for charged Higgs searches.

PACS: 12.38.-t, 14.54Ha

Keywords: top-quark, rare decay, charged Higgs

1. Introduction

The physics of the top-quark is one the main areas of study in current high energy physics. Indeed almost all characteristics of the processes with top-quark can be calculated with high theoretical accuracy. The decay $t \rightarrow bW$ is by far the dominant one with the Standard Model (SM). All other decay channels have very small branching fractions and are predicted to be smaller by several orders of magnitude in the SM [1, 2].

On the other hand, rare decays of the t -quark are very sensitive to the manifestation of New Physics beyond the SM. A very well known example is top-quark decays due to anomalous flavor changing neutral currents [1].

In this article we study a rare top-quark decay:

$$t \rightarrow bW^+\bar{b}b$$

as well as the charged Higgs boson contribution to this decay. It is shown that this decay has well identified final states and has the relatively large branching fraction, $\text{Br}(t \rightarrow b\bar{b}bW^+) \sim \mathcal{O}(10^{-3})$. We demonstrate that this four-body decay channel provides an additional way to search for charged H^\pm -boson.

Charged Higgs bosons appear in the scalar sector of several SM extensions, and is the object of various beyond the Standard Model searches at the LHC. In this article we explore a generic two-Higgs-doublet model (2HDM), which is one of the simplest SM extensions featuring a charged scalar [3, 4]. Within this class of models, two isospin doublets are introduced to break the $SU(2) \times U(1)$ symmetry, leading to the existence of five physical

Email address: Sergei.Slabospitskii@ihep.ru (S. Slabospitskii)

Higgs bosons, two of which are charged particles (H^\pm). The latest constraints the allowed H^\pm mass range as a function of $\tan\beta$ can be found in [5, 6].

Searches for H^\pm have been performed at LEP [7], at the Fermilab Tevatron [8, 9]. The ATLAS and CMS Collaborations have covered several H^\pm decay channels, such as $\tau\nu_\tau$, tb , cs , cb (see [10–16] and references therein). Note, that H^\pm -boson (like a SM Higgs) has couplings proportional to fermion masses.

The large value of the $tH^\pm b$ coupling leads to the fact that processes involving top quarks are considered for the charged Higgs production processes. The experiments explore three scenarios for the search for a charged Higgs boson. For “light” H^\pm -boson ($M(H^\pm) < m_t$) top-quark decay channel into charged Higgs is used. For the case when $M(H^\pm)$ is greater than t -quark mass, it is considered the charged Higgs production with subsequent decay into $t\bar{b}$ state. As a result the charged Higgs with masses

$$M(H^\pm) < 160 \text{ GeV} \quad \text{and} \quad M(H^\pm) > 180 \text{ GeV} \quad (1)$$

with a wide range of $\tan\beta$ are excluded [10–16].

The third scenario explores the production of the Higgs boson in association with a top quark (see [11]) with subsequent $H^\pm \rightarrow \tau^\pm\nu_\tau$ decay. As a result, the charged Higgs with mass range (90 – 2000) GeV and $\tan\beta \gtrsim 1$ is excluded.

Note, that in all experiments, a search is made for the direct production of charged Higgs with subsequent decays in observed fermions. In the present articles we propose an additional “indirect” way for H^\pm searches by study of a rare four-body top-quark decay channel ($t \rightarrow bW^+b\bar{b}$). It is shown, that t -quark decay ($t \rightarrow bW^+b\bar{b}$) provides a reasonable possibility to detect charged Higgs contribution.

Bearing in mind the experimental constraint (1) in the present article we investigate the role of the charged H^\pm -boson with mass range and $\tan\beta$ as follows:

$$M(H^\pm) = (160 \div 180) \text{ GeV} \quad \text{and} \quad \tan\beta \lesssim 1 \quad (2)$$

Throughout of this article we follow [17] for the notations, the SM vertices and SM parameters. For numerical calculations of the decay widths and production processes the C++ version of the TopReX package [18] is used. All calculations were done the following quark masses:

$$\begin{aligned} m_d &= 0.33 \text{ GeV}, & m_u &= 0.33 \text{ GeV}, \\ m_s &= 0.5 \text{ GeV}, & m_c &= 1.5 \text{ GeV}, \\ m_b &= 4.8 \text{ GeV}, & m_t &= 172.5 \text{ GeV}, \end{aligned} \quad (3)$$

We explore the b -jet tagging with b -quark identification efficiency of 70%, with probability to misidentify c quark, and light-flavor quark and gluon jets as b -jets of approximately 10% and 1%, respectively (see, e.g [19]):

$$\epsilon_b = 0.7, \epsilon_c = 0.1, \epsilon_{q, g} = 0.01 \quad (4)$$

The article is organized as follows. Charged Higgs interaction model is described in the Section 2. The constraints on $\tan\beta$ evaluated with taking into account for t -quark total decay width, as well as the branching fractions of t -quark decays, is presented in the Section 3. The width of the top-quark decay $t \rightarrow b\bar{b}W$ is calculated in the Section 4. A brief comment on t -quark decay to a multilepton final state is given in the Section 5. The different background sources are considered in the Sections 6 and 7. The kinematic of the decay $t \rightarrow b\bar{b}W^+$ is discussed in the Section 8. The last Section 9 summarize the obtained results.

2. Charged Higgs interaction Lagrangian

The interaction Lagrangian describing the H^\pm -boson-fermions interactions in the MSSM is (see [1], [4], [3]):

$$\mathcal{L} = \frac{g}{\sqrt{2}M_W} H^+ \{V_{ud}\bar{u}(m_u \cot \beta P_L + m_d \tan \beta P_R)d + \bar{\nu}(\tan \beta m_\ell P_R)\ell\}, \quad (5)$$

where $P_{L/R} = \frac{1}{2}(1 \mp \gamma^5)$, symbols u and d stand for "up" (u, c, t) and "down" (d, s, b) quarks, ν and ℓ for neutrino and charged leptons, V_{ud} is the Cabibbo-Kobayashi-Maskawa matrix element.

At tree level the corresponding decay widths are equal to [1]:

$$\Gamma(H^+ \rightarrow l\nu) = \frac{g^2 M_H}{32\pi M_W^2} m_l^2 \tan^2 \beta \quad (6)$$

$$\Gamma(H^+ \rightarrow q\bar{q}) = \frac{3g^2}{32\pi M_W^2 M_H} |V_{q\bar{q}}|^2 \lambda^{1/2} \left(1, \frac{m_q^2}{M_H^2}, \frac{m_{\bar{q}}^2}{M_H^2}\right) \times \\ [(M_H^2 - m_q^2 - m_{\bar{q}}^2)(m_q^2 \cot^2 \beta + m_{\bar{q}}^2 \tan^2 \beta) - 4m_q^2 m_{\bar{q}}^2] \quad (7)$$

$$\Gamma(t \rightarrow bH^+) = \frac{g^2}{64\pi M_W^2 m_t} |V_{tb}|^2 \lambda^{1/2} \left(1, \frac{m_b^2}{m_t^2}, \frac{M_H^2}{m_t^2}\right) \times \\ [(m_t^2 + m_b^2 - M_H^2)(m_t^2 \cot^2 \beta + m_b^2 \tan^2 \beta) + 4m_t^2 m_b^2] \quad (8)$$

where

$$\lambda(a, b, c) = a^2 + b^2 + c^2 - 2(ab + ac + bc)$$

Note, that for small $\tan \beta$ the additional decay channel ($H^+ \rightarrow t^* \bar{b} \rightarrow W^+ b \bar{b}$) can get a noticeable contribution to the total charged Higgs decay width [20] (see diagram in Fig. 1).

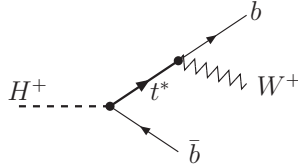


Figure 1: Diagram describing $H^+ \rightarrow t^* \bar{b} \rightarrow W^+ b \bar{b}$ decay due to virtual t -quark contribution.

In the Fig. 2 we present the behavior of the branching fractions for three H^\pm decay modes ($c\bar{s}$, $\tau\nu_{\tau\mu}$, $b\bar{b}W$) for four values of m_{H^\pm} versus $\tan \beta$. As it seen for small m_{H^\pm} values ($m_{H^\pm} \sim 100$ GeV) this three-body decay ($H^+ \rightarrow b\bar{b}W^+$) is almost negligible. Consequently, for these m_{H^\pm} -values one expects $H^+ \rightarrow \tau^+\nu$ (favoured for large $\tan \beta$) and/or $H^+ \rightarrow c\bar{s}$ (favoured for small $\tan \beta$) to be the dominant decays.

On the other hand, if $\tan \beta \lesssim 2$ and $m_{H^\pm} \gtrsim 150$ GeV, the large mass (or coupling) of the t -quark causes $\text{Br}(H^+ \rightarrow b\bar{b}W^+)$ to exceed $\text{Br}(H^+ \rightarrow c\bar{s})$. Moreover, for $\tan \beta < 1$ this three-body decay mode become dominant [1, 20] (see Fig. 2).

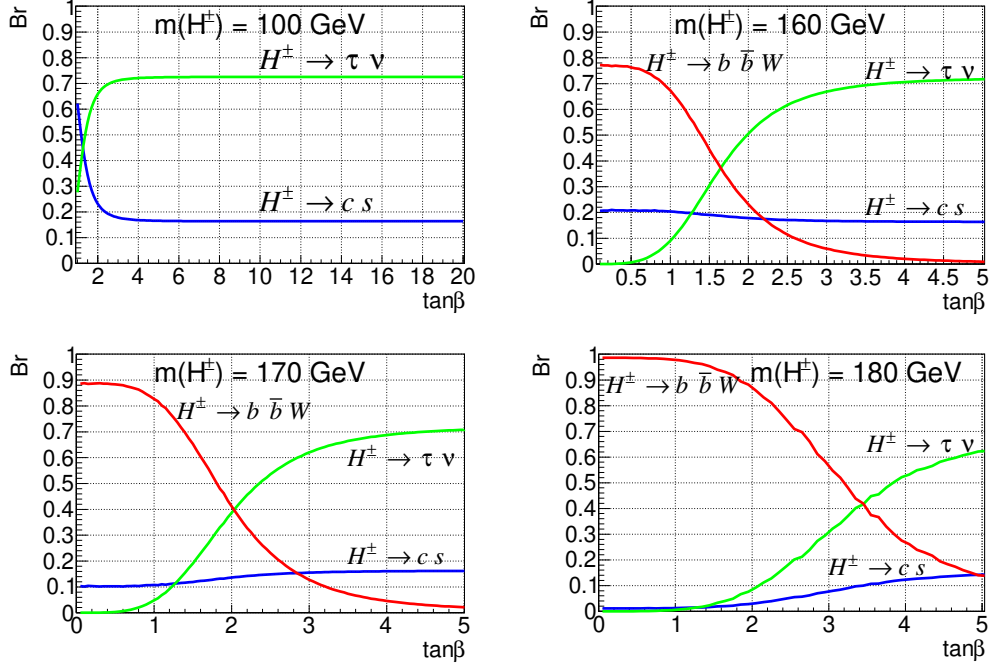


Figure 2: Branching fractions for three H^\pm decay modes for four values of m_{H^\pm} vs. $\tan\beta$.

3. Constraints on charged Higgs parameters

As explained in the introduction, we consider the charged Higgs boson with mass from 160 GeV to 180 GeV and small values of $\tan\beta$ (this area has not yet been studied in detail in the experiments).

In this section we present very rough estimates for the limits of the allowed region of $\tan\beta$ values. The charged Higgs (if it exists) should make a contribution into the total t -quark decay width as well as to the branching fractions. These values are taken from ‘‘Review of Particle Properties’’ [2]).

$$\Gamma_t = 1.42^{+0.19}_{-0.15} \text{ GeV} \quad (9)$$

$$\text{Br}(t \rightarrow bq\bar{q}) = (66.5 \pm 1.4)\% \quad (10)$$

$$\text{Br}(t \rightarrow b\tau\nu_\tau) = (11.1 \pm 0.9)\% \quad (11)$$

The first constraints could be obtained from requirement that the contribution to the total top-quark decay width could not exceed $\Delta\Gamma_t^H \approx 0.2 \text{ GeV}$. Additional constraints could be deduced by using of the top-quark branching fractions (10) and (11).

Using the errors of these branching fractions we require that charged Higgs contribution to branching fractions of these decays ($t \rightarrow bq\bar{q}$ and $t \rightarrow b\tau\nu_\tau$) should be less than the errors

from (10-11). Therefore, we explore the constraints as follows:

$$(1) \quad \Delta\Gamma_t^H < 0.2 \text{ GeV} \quad (12)$$

$$(2) \quad \left. \begin{aligned} \Delta\text{Br}^{(H)}(t \rightarrow bq\bar{q}) &= \frac{\Gamma^{(H)}(t \rightarrow bq\bar{q})}{\Gamma_{LO} + \Gamma^{(H)}(t \rightarrow bH^+)} < 0.014 \\ \Delta\text{Br}^{(H)}(t \rightarrow b\tau\nu_{\text{tau}}) &= \frac{\Gamma^{(H)}(t \rightarrow bq\bar{q})}{\Gamma_{LO} + \Gamma^{(H)}(t \rightarrow bH^+)} < 0.009 \end{aligned} \right\} \quad (13)$$

where Γ_{LO} is t -quark decay width evaluated at the leading order: $\Gamma_{LO} = \Gamma(t \rightarrow bW^+) = 1.47 \text{ GeV}$ [1]

The resulted allowed parameter ranges are presented in the Table 1 and in Fig. 3. It follows from this table and figure that the more “narrow” limits are resulted from the branching fraction constraints.

Table 1: The allowed charged Higgs parameters range. The symbols (1) and (2) corresponds to the constraints (12) and (13). The mass of H^\pm -boson is in GeV.

$M(H^\pm)$	$\tan\beta$		$M(H^\pm)$	$\tan\beta$	
	(1)	(2)		(1)	(2)
120	1.50 ÷ 24.	-	160	0.37 ÷ 93	0.55 ÷ 30.
125	1.4 ÷ 27.	5.9 ÷ 6.1	165	0.20 ÷ 115	0.26 ÷ 47
130	1.27 ÷ 29.	5. ÷ 8.	170	0.05 ÷ 135	0.089 ÷ 74
140	0.98 ÷ 37	3.3 ÷ 10.7	175	0.045 ÷ 150	0.079 ÷ 84
150	0.70 ÷ 52	2.0 ÷ 15.8	180	0.032 ÷ 165	0.071 ÷ 92

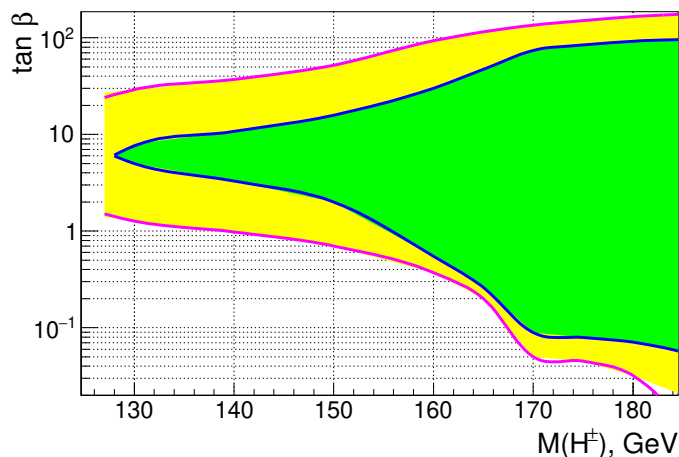


Figure 3: The allowed charged Higgs parameters range. The wide area correspond to the constraint (12), while the small one is resulted by using of the constraints (13).

Table 2: The total charged Higgs boson decay width $\Gamma_{tot}(H^\pm)$

$\tan \beta$	160	165	170	175	180
0.1	-	-	0.62	1.18	6.96
0.2	-	-	0.154	0.30	1.75
0.35	-	0.031	0.051	0.096	0.051
0.5	0.010	0.0154	0.025	0.048	0.028
1	0.0028	0.004	0.0065	0.0132	0.022
10	0.046	0.047	0.049	0.051	0.058
50	-	1.18	1.22	1.26	1.51

Certainly, these results should be considered as very rough estimates. To get more correct results one needs to take into account the NLO calculations and the running masses of the quarks.

Moreover, we do not compare these limits (see Table 1) with results from [5, 6], because, in fact, we use a rather narrow "working" area of $\tan \beta$ parameter (see Section 4 and Fig. 5). We use these range for $M(H^\pm)$ (2) and $\tan \beta$ in further calculations. In addition, for illustration, we present the total decay widths of the charged Higgs boson $\Gamma_{tot}(H^\pm)$ calculated within these limits (see Table 2).

4. Top-quark decay $t \rightarrow b W^+ b \bar{b}$

In this article we consider charged Higgs contribution to rare four-body top-quark decay:

$$t \rightarrow b W^+ b \bar{b} \quad (14)$$

Within SM this decay process is described by 28 Feynman diagrams (see Fig. 4). The picture (a) corresponds to three diagrams with virtual quarks q_U exchange ($q_U = t, u$ or $q_U = c$).

In the same fashion the pictures (b) and (c) correspond to eight diagrams with virtual bosons B exchange ($B = g, B = \gamma, B = Z$ or $B = H$). The picture (d) corresponds to three diagrams with virtual bosons V exchange ($V = \gamma, V = Z$ or $V = H$). The picture (h) corresponds to three diagrams with charged Higgs and with virtual quarks q_U exchange ($q_U = t, u, c$). Note, that the light virtual quarks (u and c) as well virtual photon, Z and H bosons give very small contributions to the $t \rightarrow b W^+ b \bar{b}$ decay width.

The calculated decay width and branching fraction are as follows:

$$\begin{aligned} \Gamma(t \rightarrow b W^+ b \bar{b}) &= (9.30 \pm 0.03) \times 10^{-4} \text{ GeV} \\ \text{Br}(t \rightarrow b W^+ b \bar{b}) &= (6.29 \pm 0.02) \times 10^{-4} \end{aligned} \quad (15)$$

In the Table 3 we present the results for several charged Higgs mass values. As it follows from calculations the partial decay width for three variants of the parameters ($\{M(H^+) = 160 \text{ GeV}, \tan \beta < 0.35\}$, $\{M(H^+) = 165 \text{ GeV}, \tan \beta < 0.2\}$, and $\{M(H^+) = 170 \text{ GeV},$

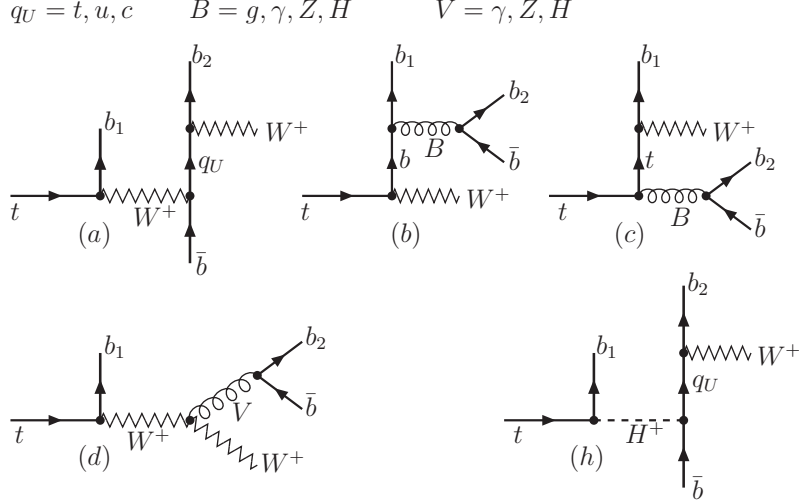


Figure 4: The diagrams((a),(b),(c) and (d)) describing $t \rightarrow bW^+ \bar{b}\bar{b}$ decay within SM. The diagram (h) describes charged Higgs contribution to this decay.

Table 3: The partial decay widths of the top-quark decay $t \rightarrow b\bar{b}W$ with account of H^\pm contribution. All width values (in GeV) are multiplied by 10^4 . The ‘‘SM’’ means that charged Higgs contribution is less the 5% and the corresponding width equals $\Gamma_{SM} \approx 9.3 \times 10^{-4}$ GeV. For $\tan\beta > 50$ and $M_H \geq 170$ GeV the decay widths are equal to Γ_{SM}

$\tan\beta$	160	165	170	175	180	185
0.1	-	-	282 ± 2.4	122 ± 1.2	75.1 ± 0.6	50.6 ± 0.4
0.2	-	-	$28.6 \pm 0.0.2$	17.7 ± 0.23	14.5 ± 0.20	13.1 ± 0.20
0.25	-	1631 ± 211	17.8 ± 0.13	13.1 ± 0.1	11.7 ± 0.09	11.0 ± 0.09
0.5	1110 ± 340	388 ± 47	10.3 ± 0.19	SM	SM	SM
1	254 ± 84	114 ± 37	SM	SM	SM	SM
30	9.9 ± 0.09	SM	SM	SM	SM	SM
50	-	10.3 ± 0.11	SM	SM	SM	SM

$\tan\beta < 0.05\}$) is exceed value 0.2 GeV. Consequently, this parameter space range should also be excluded from our further discussion.

The Fig. 5 presents the same plot as in Fig. 3 (the allowed charged Higgs parameters range). The hatched area corresponds to cases when the charged Higgs contribution to the $t \rightarrow b\bar{b}bW^+$ decay width exceeds 5%.

There is one important comment concerning the final W -boson decay into observed particles. For W -boson decaying into lepton pair ($W \rightarrow \ell\nu$) a sharp peak near the W -boson should be expected, and the corresponding decay width is

$$\Gamma(t \rightarrow b\bar{b}b\ell\nu) = \Gamma(t \rightarrow b\bar{b}bW^+) \times \text{Br}(W^+ \rightarrow \ell^+\nu)$$

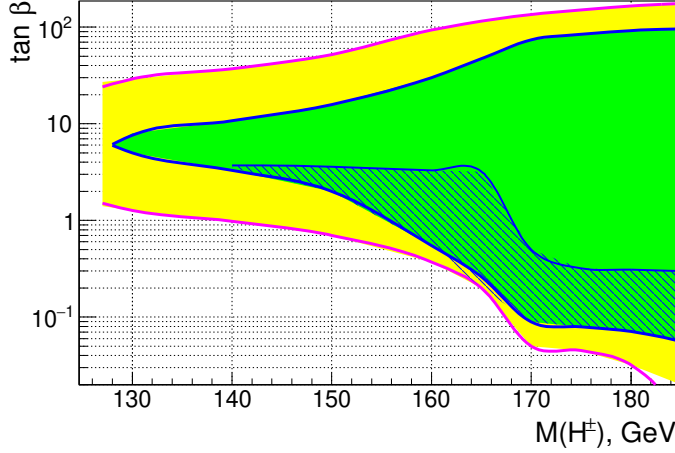


Figure 5: The same plot as in Fig. 3 (the allowed charged Higgs parameters range). The hatched area corresponds to cases when the charged Higgs contribution to the $t \rightarrow b \bar{b} b W^+$ decay width exceeds 5%.

However, this is not true for the W -boson decay into quarks. For example, there are additional diagrams, where the $c \bar{s}$ pair is produced not from W -boson (see Fig. 6).

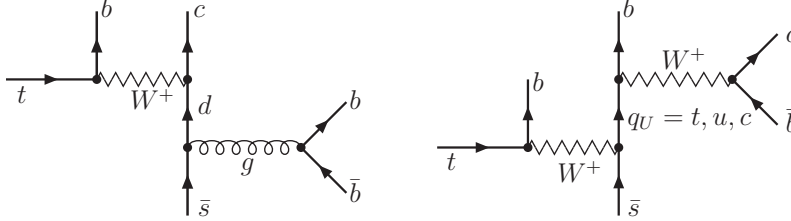


Figure 6: The representative diagrams describing the contribution to $t \rightarrow b \bar{b} b c \bar{s}$ decay, where the $c \bar{s}$ pair is not from the W -boson.

Here we present few details concerning top-quark decay channel: $t \rightarrow b \bar{b} b c \bar{s}$. The Fig. 7 presents the distribution over the invariant mass of the $c \bar{s}$ pair in the $t \rightarrow b \bar{b} b c \bar{s}$ decay.

As it follows from calculations, the contribution to the decay width from this “non-resonant” (i.e. $c \bar{s}$ is not from the W^* -boson) region approximately coincides with the contribution from $W \rightarrow q \bar{q}'$ region. As a result, the decay width of the 5-body top-quark decay channel is approximately twice the $t \rightarrow b \bar{b} b W$ decay width:

$$\begin{cases} \Gamma(t \rightarrow b \bar{b} b \ell^+ \nu) &= (1.0 \pm 0.2) \times 10^{-4} \text{ GeV} \\ \Gamma(t \rightarrow b \bar{b} b c \bar{s}) &= (6.8 \pm 0.7) \times 10^{-4} \text{ GeV} \end{cases}$$

$$\Rightarrow \Gamma(t \rightarrow b \bar{b} b f \bar{f}') = 3\Gamma(\dots \ell^+ \nu) + 2\Gamma(\dots c \bar{s}) = (16.6 \pm 1.0) \times 10^{-4} \text{ GeV} \quad (16)$$

Therefore, the decay width value (16) is about twice as large than $\Gamma(t \rightarrow b \bar{b} b W^+) = 9.3 \times 10^{-4} \text{ GeV}$ from (15).

This circumstance should be taken into account when searching for such a rare decay of the top quark. Therefore, we think that the most efficient way is the search for this decay in

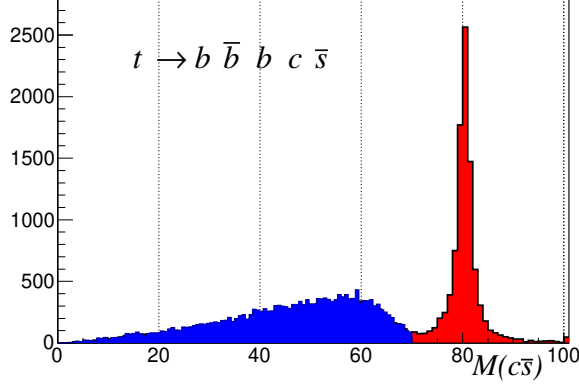


Figure 7: The distribution over the invariant mass of the $c\bar{s}$ pair in the $t \rightarrow b\bar{b}b c\bar{s}$ decay. The right sharp peak corresponds to virtual W -boson decay into $c\bar{s}$ pair, while the left wide region corresponds to the case when the $s\bar{s}$ pair is not from the W -boson.

lepton mode $t \rightarrow b\bar{b}b\ell^+\nu$. Therefore, in what follows the decay of the W -boson into leptons will be assumed in this article.

5. Top-quark decay $t \rightarrow \ell_1^+ \ell_1^- \ell_2^+ \nu_2$

It was established many years ago, that at tree level, the decay $t b Z W$ has some peculiar features, since the process occurs near the kinematic threshold ($m_t \sim M_Z + M_W + m_b$) [21–27]. A brief discussion of this decay channel can be found also in [1]. Note, that charged Higgs (at large $\tan\beta$ values) should also make a significant contribution to the top-quark decay into four leptons:

$$t \rightarrow b Z^*(\ell_1^+ \ell_1^-) W^{+*}(\ell_2^+ \nu_2) + b Z^*(\ell_1^+ \ell_1^-) \widetilde{H}^{+*}(\ell_2^+ \nu_2) \quad (17)$$

where \widetilde{H}^{+*} corresponds to all charged Higgs contributions, like $t \rightarrow b H^{+*}(\rightarrow \ell_1^+ \ell_1^- \ell_2^+ \nu_2)$, $t \rightarrow b Z^* H^{+*}(\rightarrow \ell_2^+ \nu_2)$, ...

Here, for the sake of completeness, we recalculate the width of this decay. The results of calculations for the SM case and taking into account the H^\pm -boson contribution, are given in the Table 4.

Table 4: The partial widths for $t \rightarrow b\ell_1^+ \ell_1^- \ell_2^+ \nu_2$ decay. All width values (in GeV) are multiplied by 10^8 .

$M(H^\pm), \tan\beta$	$\mu^+ \mu^- e^+ \nu_e$	$\mu^+ \mu^- \tau^+ \nu_\tau$	$\tau^+ \tau^- \mu^+ \nu_\mu$	$\tau^+ \tau^- \tau^+ \nu_\tau$
SM	6.1 ± 0.3	6.1 ± 0.3	6.1 ± 0.3	5.7 ± 0.24
160, 30	6.13 ± 0.4	11.8 ± 0.9	$28. \pm 4.$	$34.7 \pm 3.$
170, 75	6.23 ± 0.5	7.6 ± 0.5	14.9 ± 0.7	17.4 ± 0.6

As can be seen from this table, for large values of $\tan\beta$ the H^\pm -boson decay into τ -leptons gives a noticeable contribution to this partial width. However, the branching fraction is too small to for experimental searches and will not be considered further.

6. Backgrounds 1. Four-body top-decays

In this section the main sources of the background processes to the investigated decay $t \rightarrow bW^+b\bar{b}$ are discussed. We consider two types of background processes: top-quark decay into other final states and $t\bar{t}$ production in hadronic collisions accompanied by others partons (for example $pp \rightarrow t\bar{t}b\bar{b}$).

We start with the other four-body top-quark decay channels:

$$t \rightarrow bW^+ gg \text{ and } t \rightarrow bW^+ q\bar{q}' \quad (18)$$

There are about 30 decay channels with $(Wq_1\bar{q}_2q_3)$ final state and three decay channels with gluons: $t \rightarrow qggW^+$, $q = d, s, b$. The most part of these decays have very small decay widths. Therefore, we present the results for such decays that have widths at least 10% of the $t \rightarrow bWb\bar{b}$ decay width. The values of the calculated widths are given in the Table 5.

Table 5: The partial widths for $t \rightarrow bW\bar{q}_1q_2(gg)$ decay channels. The widths are in GeV. The values in third column are evaluated with requirement that invariant mass of any two particle in the final state should be greater then 20 GeV. The fourth column (“ratio”) presents the ratios of the corresponding decay widths to the $\Gamma(bWb\bar{b})$ width, taking into account the b -tagging efficiency from (4).

$t \rightarrow bW^+ \dots$	no cuts	$M(ij) > 20 \text{ GeV}$	ratio
$b\bar{b}$	$(9.30 \pm 0.03) \times 10^{-4}$	$(1.34 \pm 0.03) \times 10^{-4}$	1
gg		$(1.8 \pm 0.04) \times 10^{-3}$	0.003
$c\bar{c}$	$(4.2 \pm 0.3) \times 10^{-3}$	$(1.3 \pm 0.3) \times 10^{-4}$	0.02
$s\bar{s}$	$(1.1 \pm 0.15) \times 10^{-2}$	$(1.3 \pm 0.3) \times 10^{-4}$	0.0002
$d\bar{d} (u\bar{u})$	$(1.6 \pm 0.4) \times 10^{-2}$	$(1.3 \pm 0.3) \times 10^{-4}$	0.0002

As it seen from third column of this table the decay widths of these channels are comparable (or even greater) then the width of the main process $\Gamma(t \rightarrow b\bar{b}bW^+) = 9.3 \times 10^{-4} \text{ GeV}$ from (15). However, the b -tagging application provides a substantial suppression of the background decay channels (see fourth column in the Table 5).

7. Backgrounds 2. The production processes

In this section we consider the backgrounds from $t\bar{t}$ hadronic production accompanied by two partons:

$$pp \rightarrow t\bar{t}j_1j_2, \quad j_1j_2 = b\bar{b}, \quad gg, \quad gq, \quad q\bar{q}' \quad (19)$$

As it shown latter the main background comes from $t\bar{t}b\bar{b}$ production in pp -collisions. For pp -collisions at $\sqrt{s} = 13 \text{ TeV}$ the cross-section values were calculated [28–34] and were measured by the ATLAS and CMS Collaborations [10, 13, 35].

Following these results (for $t\bar{t}b\bar{b}$) for further calculations we use the values for cross section production of $t\bar{t}$ reaction ($\sigma(t\bar{t}) = 803 \pm 2(\text{stat}) \pm 25(\text{syst}) \pm 20(\text{lumi})$ pb (see [36] and reference therein) and for $t\bar{t}b\bar{b}$ process

$$\left. \begin{aligned} \sigma(t\bar{t}) &= 800 \text{ pb} \\ \sigma(t\bar{t}b\bar{b}) &= 4 \text{ pb} \end{aligned} \right\} \quad (20)$$

The evaluated cross-section production values for reactions (19) at $\sqrt{s} = 13$ TeV are given in Table 6 below. These values are evaluated with the following kinematic cuts:

$$p_{\top}(j) \geq 20 \text{ GeV}, \quad M(j_1 j_2) \geq 20 \text{ GeV} \quad (21)$$

As it seen the requirement to have two b -tagged jets ($jj \rightarrow (b\text{-tagging}) \rightarrow j_b j_b$) provides the substantial suppression of the all background processes except the $pp \rightarrow t\bar{t}b\bar{b}$ production.

Table 6: The cross section values for the processes $pp \rightarrow t\bar{t}j_1 j_2$ (where j stands for quarks or gluon) with kinematic cuts $p_{\top}(j) \geq 20$ GeV and $M(j_1 j_2) \geq 20$ GeV. The third column presents cross section values times b -tagging efficiencies: $\epsilon_b = 0.7, \epsilon_c = 0.1, \epsilon_q, g = 0.01$ from (4).

<i>reaction</i>	σ (pb)	$\sigma \times \epsilon_1 \epsilon_2$ (pb)	$\sigma/\sigma(t\bar{t}b\bar{b})$
$pp \rightarrow t\bar{t}b\bar{b}$	0.76 ± 0.08	0.372 ± 0.040	1
$pp \rightarrow t\bar{t}g g$	57.3 ± 12.8	$(5.73 \pm 1.28) \times 10^{-3}$	1.5×10^{-2}
$pp \rightarrow t\bar{t}u\bar{u}$	0.61 ± 0.08	$(6.1 \pm 0.8) \times 10^{-5}$	1.6×10^{-3}
$pp \rightarrow t\bar{t}uu$	0.64 ± 0.28	$(6.4 \pm 2.8) \times 10^{-5}$	1.7×10^{-4}
$pp \rightarrow t\bar{t}d\bar{d}$	0.53 ± 0.08	$(5.3 \pm 0.8) \times 10^{-5}$	1.4×10^{-3}
$pp \rightarrow t\bar{t}dd$	0.26 ± 0.2	$(2.6 \pm 2.) \times 10^{-5}$	7.0×10^{-5}
$pp \rightarrow t\bar{t}c\bar{c}$	0.56 ± 0.11	$(5.6 \pm 1.0) \times 10^{-3}$	1.5×10^{-2}
$pp \rightarrow t\bar{t}b g$	0.37 ± 0.14	$(3.7 \pm 0.14) \times 10^{-3}$	1.0×10^{-2}
$pp \rightarrow t\bar{t}\bar{b} g$	0.44 ± 0.12	$(4.4 \pm 1.2) \times 10^{-3}$	1.2×10^{-2}

Thus, the main background process comes from the $t\bar{t}b\bar{b}$ production in pp -collisions. This background can be suppressed by applying kinematic cuts to the final partons. Indeed, the processes of $t\bar{t}$ production with the subsequent four-body top-quark decay and $t\bar{t}b\bar{b}$ production have the same final state:

$$pp \rightarrow t(\rightarrow b\bar{b}W^+) \bar{t}(\rightarrow \bar{b}W^-) \rightarrow b\bar{b}bW^+\bar{b}W^- \quad (22)$$

$$pp \rightarrow t(\rightarrow bW^+) \bar{t}(\rightarrow \bar{b}W^-) b\bar{b} \rightarrow b\bar{b}bW^+\bar{b}W^- \quad (23)$$

In what follows the b -quark and \bar{b} -quark will be considered as a b -jet. Therefore, the reactions have to following (identical) final states: $4j_b W_1 W_2$. The pair j_b and W , with a mass closest to the mass of the top quark is treated as a top-quark decaying into b and W . The system consisting of the remaining particles (three b -jets and W), is considered as “top”-quark T_{3b} . Inside this T_{3b} -system we select a pair of j_b and W with maximum mass. This pair is treated as a “virtual top-quark” (t^*).

Note, that the distributions over the invariant masses of two and three b -quarks and the virtual top mass are very different for the reactions (22) and (23). The final state $3j_b W$ in the reaction (22) has a sharp peak (due to top-quark decay). These distributions are presented in the Figs. 8.

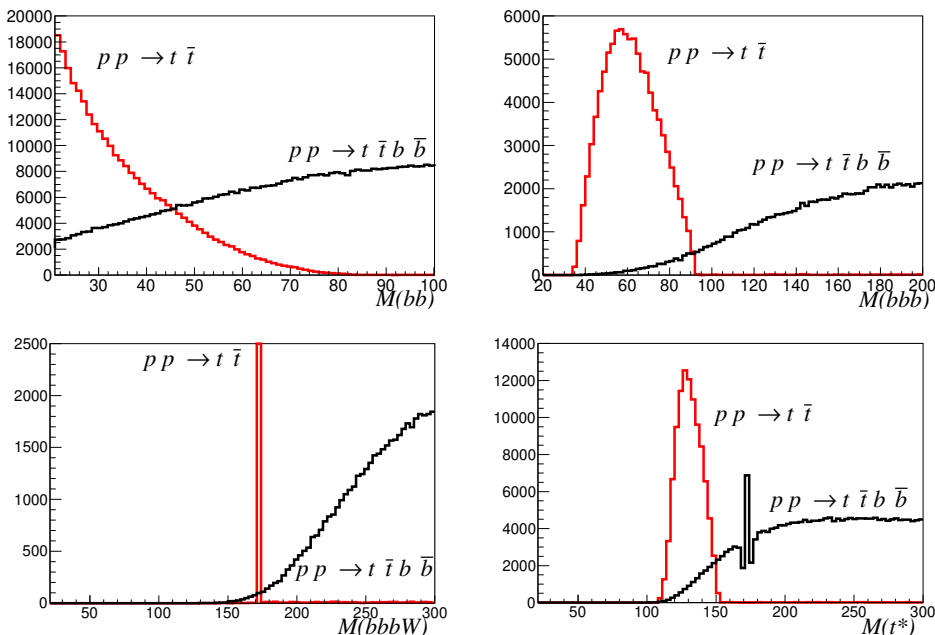


Figure 8: dN/M_{inv} distributions. The mass of two (three) b -quarks is shown in top left (top right) plot. The distributions over $3j_b W$ (virtual top t^*) is shown in the bottom left (bottom right) plot.

Therefore, to suppress the background from $t\bar{t}b\bar{b}$ production (23) we apply the kinematic cuts as follows:

$$\left. \begin{aligned} M(j_1 j_2) &\geq 20 \text{ GeV}, & p_{\top}(j) &\geq 20 \text{ GeV} \\ M(j_b j_b) &\leq 60 \text{ GeV}, & M(3j_b) &\leq 90 \text{ GeV} \\ M(3j_b W) &\leq 200 \text{ GeV}, & M(t^*) &= 100 \div 150 \text{ GeV} \end{aligned} \right\} \quad (24)$$

After applying of all cuts from (24) the total efficiencies (ϵ_{cuts}) of event detection for the $T_{3b}(b\bar{b}bW)$ system are as follows:

$$\left. \begin{aligned} pp \rightarrow t\bar{t} &: \epsilon_{cuts} = 0.086 \\ pp \rightarrow t\bar{t}b\bar{b} &: \epsilon_{cuts} = 0.00034 \end{aligned} \right\} \quad (25)$$

As a result the application of all cuts (24) provides a rather well suppression of the background process:

$$R = \frac{\sigma(t\bar{t}b\bar{b}) \times \epsilon_{cuts}}{\sigma(t\bar{t}) \times \epsilon_{cuts} \times \text{Br}(t \rightarrow 3bW)} = 0.031 \quad (26)$$

where $\sigma(t\bar{t}b\bar{b})$ and $\sigma(t\bar{t})$ are taken from (20). Therefore, in what follows we consider the signal process (22) only.

Then, for estimation the expected number of events we use the following options:

- the LHC Run-3 integrated luminosity equals $L_{tot} = 300 \text{ fb}^{-1}$;
- $\text{Br}(t \rightarrow b\bar{b}W) = 6.29 \times 10^{-4}$;
- the kinematic cuts from (24);
- W^+W^- decay into $\ell\nu$ and $q\bar{q}'$: $W^+W^- \rightarrow e(\mu)\nu q\bar{q}'$.

As a result, at LHC Run-3 option the expected number of events for $t\bar{t}$ -pair production with subsequent decays (with the following W^+W^- decays) are as follows:

$$t\bar{t} \rightarrow b\bar{b}W^+ \bar{b}W^- \rightarrow 2b2\bar{b}\ell\nu q\bar{q}'$$

$$N(2b2\bar{b}\ell\nu q\bar{q}') \approx 2000 \quad (27)$$

This number of events is large enough that the search for such rare decay looks like a promising goal for the experimental searches.

8. Kinematics

In this section we study the obvious question: *how one get a manifestation of the charged Higgs boson contribution to this rare $t \rightarrow bW^+b\bar{b}$ decay of the top-quark ?*

In this section , the symbol "SM" corresponds to the case when top-quark decays within the SM, while "H" denotes the inclusion (exchange) of charged Higgs boson:

$$t_{SM} \rightarrow b\bar{b}W^+ \quad : \quad (\text{SM only}) \quad (28)$$

$$t_H \rightarrow b\bar{b}W^+ \quad : \quad (\text{SM} + H^\pm) \quad (29)$$

As it seen from the Table 3 for a small $\tan\beta$ values ($\tan\beta \leq 0.2$) the decay width due to H^\pm contribution exceeds the SM value by at least one (or even two) order of magnitude.

Therefore, one could expect a significant increase in the number of events in this case. Additional manifestation of the H^\pm contribution can be seen in different kinematic distributions. We have found one variable, whose distribution demonstrates clear difference in decays (28) and (29). This is the cosine of the angle between the 3-momenta of the final b -quarks in the t -quark rest frame, $\cos\theta_{bb}$. These distributions are shown in the Figs. 9 and 10.

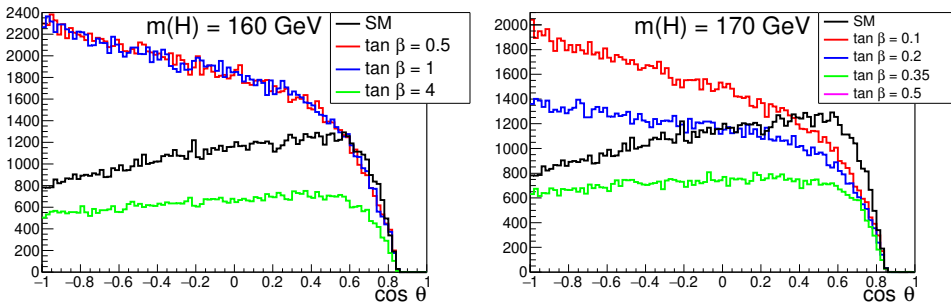


Figure 9: The distribution over $\cos\theta_{bb}$ for two charged Higgs masses and for several $\tan\beta$ values. The black curve corresponds to SM $t \rightarrow b\bar{b}W^+$ decay.

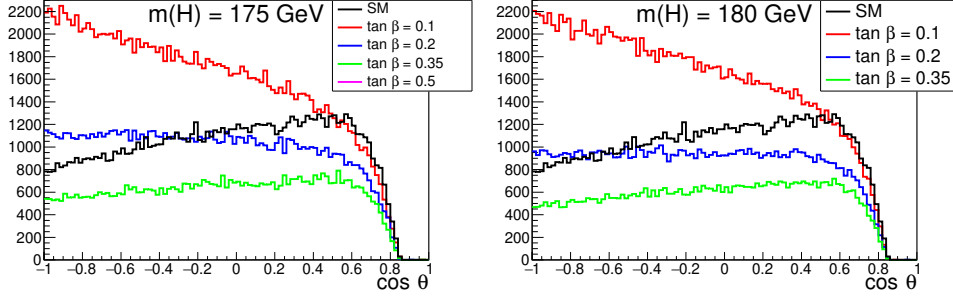


Figure 10: The same distributions as in Fig. 9, but for $M(H^\pm) = 175$ and 180 GeV.

As can be seen from these plots, for small $\tan\beta$ values ($\tan\beta \leq 0.2$) these distributions for t_H decay (29) have a shape different from the SM decay.

The next plots (see Fig. 11) present the same distributions, but evaluated for top-quark production in pp -collisions at $\sqrt{s} = 13$ TeV after application all cuts from (24). It is seen an obvious difference in distributions over $\cos\theta_{bb}$.

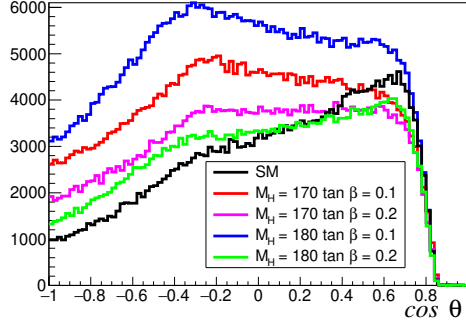


Figure 11: The distribution over $\cos\theta_{bb}$ for for-body top-quark decay. Here the t -quark is produced in pp -collisions at $\sqrt{s} = 13$ TeV. The black curve corresponds to SM decay $t \rightarrow b\bar{b}bW^+$.

Certainly, this conclusion is nothing more than a demonstration of different kinematic in (28) and (29) decays. More realistic simulation could destroy this pictures and conclusions. Nevertheless, we believe that advanced methods of the experimental data analysis will make it possible to search for this rare t -quark four-body decay and (in principle) to detect manifestation of a charged Higgs boson (if it exists) to this $t \rightarrow bW^+b\bar{b}$ decay.

9. Conclusion

In this article the rare top decay $t \rightarrow b\bar{b}bW^+$ is considered. The relatively large partial decay width, $\Gamma(t \rightarrow b\bar{b}bW^+) = (9.30 \pm 0.03) \times 10^{-4}$ GeV (and $\text{Br}(t \rightarrow b\bar{b}bW^+) = 6.29 \times 10^{-4}$), makes possible the searches for this rare t -quark decay at LHC.

The role of the charged Higgs boson (with the mass $M(H^\pm) = (160 \div 180)$ GeV and $\tan\beta \lesssim 1$) in top-quark decays is considered. Taking in account the current value of the

t -quark total decay width as well as the branching fractions of t -quark decays, the allowable region of $\tan\beta$ versus $M(H^\pm)$ is evaluated.

In this article we propose an additional method for H^\pm -boson searches. This scenario explores only the increase of the partial width of the $t \rightarrow b\bar{b}bW^+$ decay and does not require the appearance of the peak in the invariant mass distributions around the mass of the charged Higgs boson.

It is shown that the H^\pm -boson contribution to $\Gamma(t \rightarrow b\bar{b}bW^+)$ with $\tan\beta \lesssim 1$ could increase this width by up to two orders of magnitude (depending on $\tan\beta$ values).

The role of the possible background processes (for t -quark decay as well as for production) is investigated. The exploration of the b -tagging ($\varepsilon_b \approx 70\%$) provides sufficiently good suppression of all other decay channels. The main background to $t\bar{t}$ production with subsequent $t \rightarrow b\bar{b}bW^+$ decay comes from four heavy quarks production ($pp \rightarrow t\bar{t}b\bar{b}$). This background also could be suppressed by exploring of b -tagging and proper kinematic cuts.

As a result one may expect to get about 2000 events at LHC energies with total luminosity of $\mathcal{L}_{tot} = 300 \text{ fb}^{-1}$ for the SM t -quark decay $t \rightarrow b\bar{b}bW^+(\rightarrow e/\mu\nu)$. Such a number of expected events makes it realistic challenge for this study is in the LHC experiments.

Acknowledgments

In conclusion the author is grateful to P.S. Mandrik, V.F. Obraztsov, R.N. Rogalyov, and A.M. Zaitsev for multiple and fruitful discussions.

References

- [1] M. Beneke, et al., Top quark physics, in: Workshop on Standard Model Physics (and more) at the LHC (First Plenary Meeting), 2000, pp. 419–529 (3 2000). [arXiv:hep-ph/0003033](#).
- [2] P. A. Zyla, et al., Review of Particle Physics, PTEP 2020 (8) (2020) 083C01, <https://pdg.lbl.gov/> (2020). [doi:10.1093/ptep/ptaa104](https://doi.org/10.1093/ptep/ptaa104).
- [3] V. D. Barger, R. J. N. Phillips, COLLIDER PHYSICS, Vol. 71, Addison-Wesley, 1987 (1987).
- [4] G. C. Branco, P. M. Ferreira, L. Lavoura, M. N. Rebelo, M. Sher, J. P. Silva, Theory and phenomenology of two-Higgs-doublet models, Phys. Rept. 516 (2012) 1–102 (2012). [arXiv:1106.0034](#), [doi:10.1016/j.physrep.2012.02.002](https://doi.org/10.1016/j.physrep.2012.02.002).
- [5] A. G. Akeroyd, et al., Prospects for charged Higgs searches at the LHC, Eur. Phys. J. C 77 (5) (2017) 276 (2017). [arXiv:1607.01320](#), [doi:10.1140/epjc/s10052-017-4829-2](https://doi.org/10.1140/epjc/s10052-017-4829-2).
- [6] A. Arbey, F. Mahmoudi, O. Stal, T. Stefaniak, Status of the Charged Higgs Boson in Two Higgs Doublet Models, Eur. Phys. J. C 78 (3) (2018) 182 (2018). [arXiv:1706.07414](#), [doi:10.1140/epjc/s10052-018-5651-1](https://doi.org/10.1140/epjc/s10052-018-5651-1).

- [7] G. Abbiendi, et al., Search for Charged Higgs bosons: Combined Results Using LEP Data, *Eur. Phys. J. C* 73 (2013) 2463 (2013). [arXiv:1301.6065](#), [doi:10.1140/epjc/s10052-013-2463-1](#).
- [8] T. Aaltonen, et al., Search for Higgs bosons predicted in two-Higgs-doublet models via decays to tau lepton pairs in 1.96-TeV p anti-p collisions, *Phys. Rev. Lett.* 103 (2009) 201801 (2009). [arXiv:0906.1014](#), [doi:10.1103/PhysRevLett.103.201801](#).
- [9] V. M. Abazov, et al., Search for Higgs bosons of the minimal supersymmetric standard model in $p\bar{p}$ collisions at $\sqrt{s} = 1.96$ TeV, *Phys. Lett. B* 710 (2012) 569–577 (2012). [arXiv:1112.5431](#), [doi:10.1016/j.physletb.2012.03.021](#).
- [10] M. Aaboud, et al., Measurements of inclusive and differential fiducial cross-sections of $t\bar{t}$ production with additional heavy-flavour jets in proton-proton collisions at $\sqrt{s} = 13$ TeV with the ATLAS detector, *JHEP* 04 (2019) 046 (2019). [arXiv:1811.12113](#), [doi:10.1007/JHEP04\(2019\)046](#).
- [11] M. Aaboud, et al., Search for charged Higgs bosons decaying via $H^\pm \rightarrow \tau^\pm \nu_\tau$ in the τ +jets and τ +lepton final states with 36 fb^{-1} of pp collision data recorded at $\sqrt{s} = 13$ TeV with the ATLAS experiment, *JHEP* 09 (2018) 139 (2018). [arXiv:1807.07915](#), [doi:10.1007/JHEP09\(2018\)139](#).
- [12] G. Aad, et al., Search for charged Higgs bosons decaying into a top quark and a bottom quark at $\sqrt{s} = 13$ TeV with the ATLAS detector, *JHEP* 06 (2021) 145 (2021). [arXiv:2102.10076](#), [doi:10.1007/JHEP06\(2021\)145](#).
- [13] A. M. Sirunyan, et al., Measurement of the $t\bar{t}b\bar{b}$ production cross section in the all-jet final state in pp collisions at $\sqrt{s} = 13$ TeV, *Phys. Lett. B* 803 (2020) 135285 (2020). [arXiv:1909.05306](#), [doi:10.1016/j.physletb.2020.135285](#).
- [14] A. M. Sirunyan, et al., Search for a light charged Higgs boson in the $H^\pm \rightarrow cs$ channel in proton-proton collisions at $\sqrt{s} = 13$ TeV, *Phys. Rev. D* 102 (7) (2020) 072001 (2020). [arXiv:2005.08900](#), [doi:10.1103/PhysRevD.102.072001](#).
- [15] A. M. Sirunyan, et al., Search for a charged Higgs boson decaying into top and bottom quarks in events with electrons or muons in proton-proton collisions at $\sqrt{s} = 13$ TeV, *JHEP* 01 (2020) 096 (2020). [arXiv:1908.09206](#), [doi:10.1007/JHEP01\(2020\)096](#).
- [16] A. M. Sirunyan, et al., Search for charged Higgs bosons decaying into a top and a bottom quark in the all-jet final state of pp collisions at $\sqrt{s} = 13$ TeV, *JHEP* 07 (2020) 126 (2020). [arXiv:2001.07763](#), [doi:10.1007/JHEP07\(2020\)126](#).
- [17] V. I. Borodulin, R. N. Rogalyov, S. R. Slabospitskii, CORE 3.1 (COmpendium of RElations, Version 3.1) (2 2017). [arXiv:1702.08246](#).
- [18] S. R. Slabospitsky, L. Sonnenschein, TopReX generator (version 3.25): Short manual, *Comput. Phys. Commun.* 148 (2002) 87–102 (2002). [arXiv:hep-ph/0201292](#), [doi:10.1016/S0010-4655\(02\)00471-X](#).

- [19] A. M. Sirunyan, et al., Identification of heavy-flavour jets with the CMS detector in pp collisions at 13 TeV, JINST 13 (05) (2018) P05011 (2018). [arXiv:1712.07158](#), [doi:10.1088/1748-0221/13/05/P05011](#).
- [20] E. Ma, D. P. Roy, J. Wudka, Enhanced three-body decay of the charged Higgs boson, Phys. Rev. Lett. 80 (1998) 1162–1165 (1998). [arXiv:hep-ph/9710447](#), [doi:10.1103/PhysRevLett.80.1162](#).
- [21] R. Decker, M. Nowakowski, A. Pilaftsis, Dominant three-body decays of a heavy Higgs and top quark, Z. Phys. C 57 (1993) 339–348 (1993). [arXiv:hep-ph/9301283](#), [doi:10.1007/BF01565067](#).
- [22] G. Mahlon, S. J. Parke, Finite width effects in top quark decays, Phys. Lett. B 347 (1995) 394–398 (1995). [arXiv:hep-ph/9412250](#), [doi:10.1016/0370-2693\(95\)00083-W](#).
- [23] E. E. Jenkins, The Rare top decays $t \rightarrow bW^+Z$ and $t \rightarrow cW^+W^-$, Phys. Rev. D 56 (1997) 458–466 (1997). [arXiv:hep-ph/9612211](#), [doi:10.1103/PhysRevD.56.458](#).
- [24] G. Altarelli, L. Conti, V. Lubicz, The $t \rightarrow WZb$ decay in the standard model: A Critical reanalysis, Phys. Lett. B 502 (2001) 125–132 (2001). [arXiv:hep-ph/0010090](#), [doi:10.1016/S0370-2693\(00\)01333-2](#).
- [25] A. Papaefstathiou, G. Tetlalmatzi-Xolocotzi, Rare top quark decays at a 100 TeV proton–proton collider: $t \rightarrow bWZ$ and $t \rightarrow hc$, Eur. Phys. J. C 78 (3) (2018) 214 (2018). [arXiv:1712.06332](#), [doi:10.1140/epjc/s10052-018-5701-8](#).
- [26] P. Onyisi, A. Webb, Impact of rare decays $t \rightarrow \ell' \nu b \ell \ell$ and $t \rightarrow q q' b \ell \ell$ on searches for top-associated physics, JHEP 02 (2018) 156 (2018). [arXiv:1704.07343](#), [doi:10.1007/JHEP02\(2018\)156](#).
- [27] N. Quintero, J. L. Diaz-Cruz, G. Lopez Castro, Lepton pair emission in the top quark decay $t \rightarrow bW^+ \ell^- \ell^+$, Phys. Rev. D 89 (9) (2014) 093014 (2014). [arXiv:1403.3044](#), [doi:10.1103/PhysRevD.89.093014](#).
- [28] A. Bredenstein, A. Denner, S. Dittmaier, S. Pozzorini, NLO QCD corrections to t anti- t b anti- b production at the LHC: 1. Quark-antiquark annihilation, JHEP 08 (2008) 108 (2008). [arXiv:0807.1248](#), [doi:10.1088/1126-6708/2008/08/108](#).
- [29] F. Cascioli, P. Maierhöfer, N. Moretti, S. Pozzorini, F. Siegert, NLO matching for $t\bar{t}b\bar{b}$ production with massive b -quarks, Phys. Lett. B 734 (2014) 210–214 (2014). [arXiv:1309.5912](#), [doi:10.1016/j.physletb.2014.05.040](#).
- [30] M. V. Garzelli, A. Kardos, Z. Trócsányi, Hadroproduction of $t\bar{t}b\bar{b}$ final states at LHC: predictions at NLO accuracy matched with Parton Shower, JHEP 03 (2015) 083 (2015). [arXiv:1408.0266](#), [doi:10.1007/JHEP03\(2015\)083](#).
- [31] G. Bevilacqua, M. Czakon, C. G. Papadopoulos, M. Worek, Hadronic top-quark pair production in association with two jets at Next-to-Leading Order QCD, Phys. Rev. D 84 (2011) 114017 (2011). [arXiv:1108.2851](#), [doi:10.1103/PhysRevD.84.114017](#).

- [32] G. Bevilacqua, M. Worek, On the ratio of $t\bar{t}b\bar{b}$ and $t\bar{t}jj$ cross sections at the CERN Large Hadron Collider, JHEP 07 (2014) 135 (2014). [arXiv:1403.2046](#), [doi:10.1007/JHEP07\(2014\)135](#).
- [33] G. Bevilacqua, M. V. Garzelli, A. Kardos, $t\bar{t}b\bar{b}$ hadroproduction with massive bottom quarks with PowHel (9 2017). [arXiv:1709.06915](#).
- [34] T. Ježo, J. M. Lindert, N. Moretti, S. Pozzorini, New NLOPS predictions for $t\bar{t} + b$ -jet production at the LHC, Eur. Phys. J. C 78 (6) (2018) 502 (2018). [arXiv:1802.00426](#), [doi:10.1140/epjc/s10052-018-5956-0](#).
- [35] A. M. Sirunyan, et al., Measurement of the cross section for $t\bar{t}$ production with additional jets and b jets in pp collisions at $\sqrt{s} = 13$ TeV, JHEP 07 (2020) 125 (2020). [arXiv:2003.06467](#), [doi:10.1007/JHEP07\(2020\)125](#).
- [36] S. Grancagnolo, Top quark pair-production cross section measurements at LHC, PoS DIS2019 (2019) 152 (2019). [doi:10.22323/1.352.0152](#).